3. B. L. Cushing, V. L. Kolesnichenko, C. J. O'Connor, *Chem. Rev.* **104**, 3893 (2004).
4. Y. Yin, A. P. Alivisatos, *Nature* **437**, 664 (2005).
5. D. J. Norris, A. L. Efros, S. C. Erwin, *Science* **319**, 1776 (2008).
6. X. G. Peng *et al.*, *Nature* **404**, 59 (2000).
7. L. Manna, E. C. Scher, A. P. Alivisatos, *J. Am. Chem. Soc.* **122**, 12700 (2000).
8. V. F. Puntes, K. M. Krishnan, A. P. Alivisatos, *Science* **291**, 2115 (2001).
9. V. F. Puntes, D. Zanchet, C. K. Erdonmez, A. P. Alivisatos, *J. Am. Chem. Soc.* **124**, 12874 (2002).
10. D. J. Milliron *et al.*, *Nature* **430**, 190 (2004).
11. Y. D. Yin *et al.*, *Science* **304**, 711 (2004).
12. V. K. LaMer, R. H. Dinergar, *J. Am. Chem. Soc.* **72**, 4847 (1950).
13. H. Reiss, *J. Chem. Phys.* **19**, 482 (1951).
14. T. Sugimoto, *Adv. Colloid Interface Sci.* **28**, 65 (1987).
15. D. V. Leff, P. C. Ohara, J. R. Heath, W. M. Gelbart, *J. Phys. Chem. B* **99**, 7036 (1995).
16. Y. Chen, E. Johnson, X. Peng, *J. Am. Chem. Soc.* **129**, 10937 (2007).
17. Y. A. Yang, H. M. Wu, K. R. Williams, Y. C. Cao, *Angew. Chem. Int. Ed.* **44**, 6712 (2005).
18. J. F. Banfield, S. A. Welch, H. Z. Zhang, T. T. Ebert, R. L. Penn, *Science* **289**, 751 (2000).
19. C. Pacholski, A. Kornowski, H. Weller, *Angew. Chem. Int. Ed.* **41**, 1188 (2002).
20. J. H. Yu *et al.*, *J. Am. Chem. Soc.* **127**, 5662 (2005).
21. M. Niederberger, H. Colfen, *Phys. Chem. Chem. Phys.* **8**, 3271 (2006).
22. M. A. Watzky, E. E. Finney, R. G. Finke, *J. Am. Chem. Soc.* **130**, 11959 (2008).
23. M. J. Williamson, R. M. Tromp, P. M. Vereecken, R. Hull, F. M. Ross, *Nat. Mater.* **2**, 532 (2003).
24. P. L. Gai, *Microsc. Microanal.* **8**, 21 (2002).
25. K. L. Liu *et al.*, *Lab Chip* **8**, 1915 (2008).
26. N. de Jonge, D. B. Peckys, G. J. Kremers, D. W. Piston, *Proc. Natl. Acad. Sci. U.S.A.* **106**, 2159 (2009).
27. Materials and methods are available as supporting material on *Science* Online.
28. F. M. Ross, J. Tersoff, R. M. Tromp, *Phys. Rev. Lett.* **80**, 984 (1998).
29. J. E. Burke, D. Turnbull, in *Progress in Metal Physics*, vol. 3 (Pergamon Press, London, 1952), pp. 220–292.
30. The authors would like to thank A. Minor and J. Turner for their help with the initial tests on the liquid cells. This project is supported by the Director, Office of Science, Office of Basic Energy Sciences, Materials Sciences and Engineering Division of the U.S. Department of Energy under contract DE-AC02-05CH11231.

Supporting Online Material
www.sciencemag.org/cgi/content/full/324/5932/1309/DC1
Materials and Methods
Figs. S1 to S3
Movies S1 and S2
References

10 February 2009; accepted 8 April 2009
10.1126/science.1172104

Large-Area Synthesis of High-Quality and Uniform Graphene Films on Copper Foils

Xuesong Li,[1] Weiwei Cai,[1] Jinho An,[1] Seyoung Kim,[2] Junghyo Nah,[2] Dongxing Yang,[1] Richard Piner,[1] Aruna Velamakanni,[1] Inhwa Jung,[1] Emanuel Tutuc,[2] Sanjay K. Banerjee,[2] Luigi Colombo,[3]* Rodney S. Ruoff[1]*

Graphene has been attracting great interest because of its distinctive band structure and physical properties. Today, graphene is limited to small sizes because it is produced mostly by exfoliating graphite. We grew large-area graphene films of the order of centimeters on copper substrates by chemical vapor deposition using methane. The films are predominantly single-layer graphene, with a small percentage (less than 5%) of the area having few layers, and are continuous across copper surface steps and grain boundaries. The low solubility of carbon in copper appears to help make this growth process self-limiting. We also developed graphene film transfer processes to arbitrary substrates, and dual-gated field-effect transistors fabricated on silicon/silicon dioxide substrates showed electron mobilities as high as 4050 square centimeters per volt per second at room temperature.

Graphene, a monolayer of sp^2-bonded carbon atoms, is a quasi–two-dimensional (2D) material. Graphene has been attracting great interest because of its distinctive band structure and physical properties (*1*). Today, the size of graphene films produced is limited to small sizes (usually <1000 μm^2) because the films are produced mostly by exfoliating graphite, which is not a scalable technique. Graphene has also been synthesized by the desorption of Si from SiC single-crystal surfaces, which yields a multilayered graphene structure that behaves like graphene (*2*, *3*), and by a surface precipitation process of carbon in some transition metals (*4*–*8*).

[1]Department of Mechanical Engineering and the Texas Materials Institute, 1 University Station C2200, The University of Texas at Austin, Austin, TX 78712–0292, USA. [2]Department of Electrical and Computer Engineering, Microelectronics Research Center, The University of Texas at Austin, Austin, TX 78758, USA. [3]Texas Instruments, Dallas, TX 75243, USA.

*To whom correspondence should be addressed. E-mail: colombo@ti.com (L.C.); r.ruoff@mail.utexas.edu (R.S.R.)

Electronic application will require high-quality large-area graphene that can be manipulated to make complex devices and integrated in silicon device flows. Field-effect transistors (FETs) fabricated with exfoliated graphite have shown promising electrical properties (*9*, *10*), but these devices will not meet the silicon device scaling requirements, especially those for power reduction and performance. One device that could meet the silicon roadmap requirements beyond the 15-nm node was proposed by S. K. Banerjee *et al.* (*11*). The device is a "BisFET" (bilayer pseudospin FET) that is made up of two graphene layers separated by a thin dielectric. The ability to create this device can be facilitated by the availability of large-area graphene. Making a transparent electrode, another promising application of graphene, also requires large films (*6*, *12*–*14*).

At this time, there is no pathway for the formation of a graphene layer that can be exfoliated from or transferred from the graphene synthesized on SiC, but there is a way to grow and transfer graphene grown on metal substrates (*5*–*7*). Although graphene has been grown on a number of metals, we still have the challenge of growing large-area graphene. For example, graphene grown on Ni seems to be limited by its small grain size, presence of multilayers at the grain boundaries, and the high solubility of carbon (*6*, *7*). We have developed a graphene chemical vapor deposition (CVD) growth process on copper foils (25 μm thick in our experiment). The films grow directly on the surface by a surface-catalyzed process, and the film is predominantly graphene with <5% of the area having two- and three-layer graphene flakes. Under our processing conditions, the two- and three-layer flakes do not grow larger with time. One of the major benefits of our process is that it can be used to grow graphene on 300-mm copper films on Si substrates (a standard process in Si technology). It is also well known that annealing of Cu can lead to very large grains.

As described in (*15*), we grew graphene on copper foils at temperatures up to 1000°C by CVD of carbon using a mixture of methane and hydrogen. Figure 1A shows a scanning electron microscopy (SEM) image of graphene on a copper substrate where the Cu grains are clearly visible. A higher-resolution image of graphene on Cu (Fig. 1B) shows the presence of Cu surface steps, graphene "wrinkles," and the presence of non-uniform dark flakes. The wrinkles associated with the thermal expansion coefficient difference between Cu and graphene are also found to cross Cu grain boundaries, indicating that the graphene film is continuous. The inset in Fig. 1B shows transmission electron microscopy (TEM) images of graphene and bilayer graphene. With the use of a process similar to that described in (*16*), the as-grown graphene can be easily transferred to alternative substrates, such as SiO_2/Si or glass (Fig. 1, C and D), for further evaluation and for various applications; a detailed transfer process is described (*15*). The process and method used to transfer graphene from Cu was the same for the SiO_2/Si substrate and the glass substrate. Al-

Downloaded from www.sciencemag.org on October 12, 2010

though it is difficult to see the graphene on the SiO_2/Si substrate, a similar graphene film from another Cu substrate transferred on glass clearly shows that it is optically uniform.

We used Raman spectroscopy to evaluate the quality and uniformity of graphene on a SiO_2/Si substrate. Figure 2 shows SEM and optical images with the corresponding Raman spectra and maps of the D, G, and 2D bands providing information on the defect density and film thickness. The Raman spectra are from the spots marked with the corresponding colored circles shown in the other panels (in Fig. 2, A and B, green arrows are used instead of circles so as to show the trilayer region more clearly). The thickness and uniformity of the graphene films were evaluated via color contrast under optical microscope (*17*) and Raman spectra (*7*, *18*, *19*).

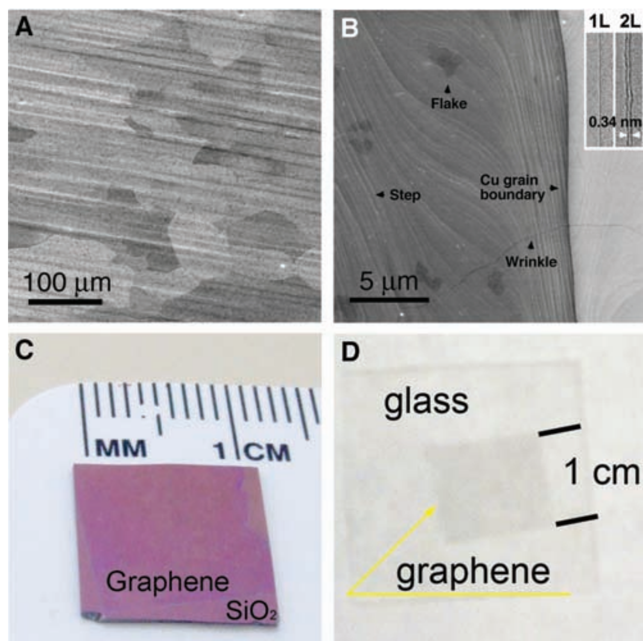

Fig. 1. (**A**) SEM image of graphene on a copper foil with a growth time of 30 min. (**B**) High-resolution SEM image showing a Cu grain boundary and steps, two- and three-layer graphene flakes, and graphene wrinkles. Inset in (B) shows TEM images of folded graphene edges. 1L, one layer; 2L, two layers. (**C** and **D**) Graphene films transferred onto a SiO_2/Si substrate and a glass plate, respectively.

The Raman spectrum from the lightest pink background in Fig. 2B shows typical features of monolayer graphene: (i) a ~0.5 G–to–2D intensity ratio and (ii) a symmetric 2D band centered at ~2680 cm^{-1} with a full width at half maximum of ~33 cm^{-1}. The second lightest pink flakes (blue circle) correspond to bilayer graphene, and the darkest one (green arrow) represents trilayer graphene. This thickness variation is more clearly shown in the SEM image in Fig. 2A. The D map in Fig. 2D, which has been associated with defects in graphene, is rather uniform and near the background level, except for regions where wrinkles are present and close to few-layer regions. The G and the 2D maps clearly show the presence of more than one layer in the flakes. In the wrinkled regions, there are peak height variations in both the G and 2D bands, and there is a broadening of the 2D band. An analysis of the intensity of the optical image over the whole sample (1 cm by 1 cm) showed that the area with the lightest pink color is more than 95%, and all 40 Raman spectra randomly collected from this area show monolayer graphene. There is only a small fraction of trilayer or few-layer (<10) graphene (<1%), and the rest is bilayer graphene (~3 to 4%).

We grew films on Cu as a function of time and Cu foil thickness under isothermal and isobaric conditions. Using the process flow described in (*15*), we found that graphene growth on Cu is self-limited; growth that proceeded for more than 60 min yielded a similar structure to growth runs performed for ~10 min. For times

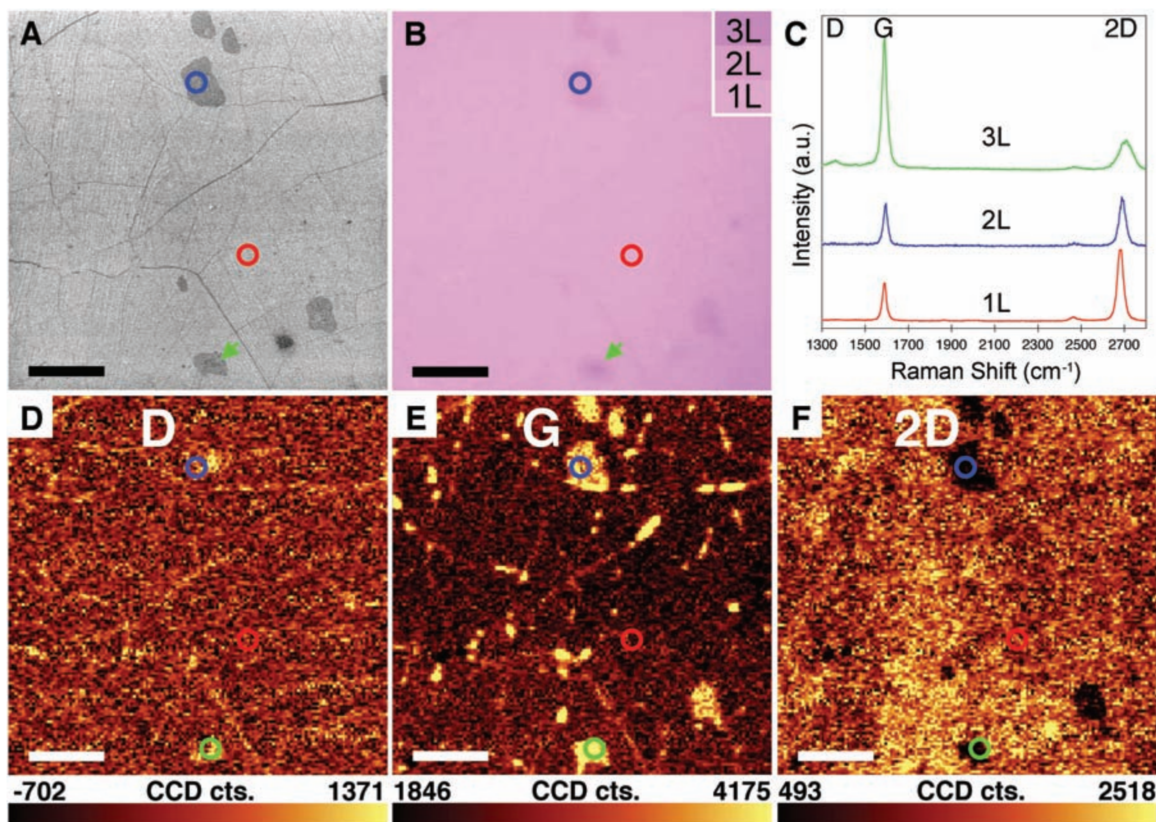

Fig. 2. (**A**) SEM image of graphene transferred on SiO_2/Si (285-nm-thick oxide layer) showing wrinkles, as well as two- and three-layer regions. (**B**) Optical microscope image of the same regions as in (A). (**C**) Raman spectra from the marked spots with corresponding colored circles or arrows showing the presence of one, two, and three layers of graphene. a.u., arbitrary units. (**D** to **F**) Raman maps of the D (1300 to 1400 cm^{-1}), G (1560 to 1620 cm^{-1}), and 2D (2660 to 2700 cm^{-1}) bands, respectively (WITec alpha300, λ_{laser} = 532 nm, ~500-nm spot size, 100× objector). CCD cts., charge-coupled device counts. Scale bars, 5 μm.

Downloaded from www.sciencemag.org on October 12, 2010

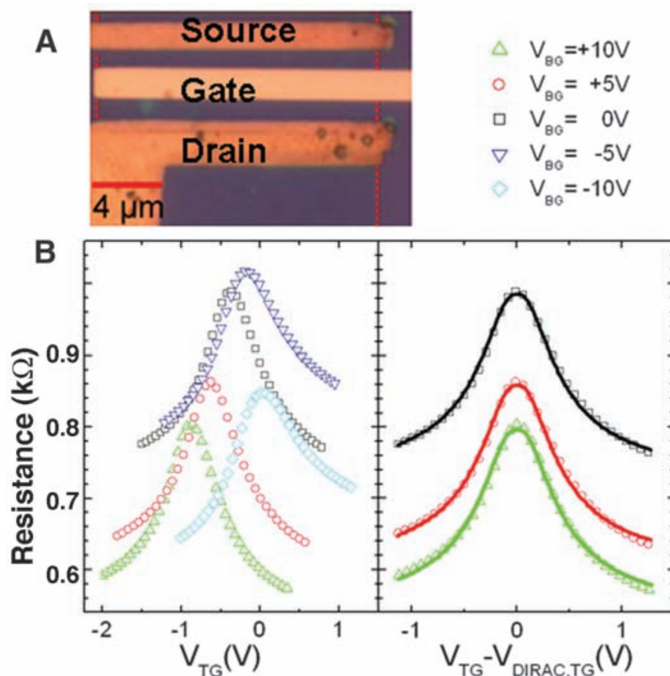

Fig. 3. (**A**) Optical microscope image of a graphene FET. (**B**) Device resistance versus top-gate voltage (V_{TG}), with different back-gate (V_{BG}) biases, and versus V_{TG}-$V_{Dirac,TG}$ (V_{TG} at the Dirac point), with a model fit (solid line).

much less than 10 min, the Cu surface is usually not fully covered [SEM images of graphene on Cu with different growth time are shown in fig. S3 (*15*)]. The growth of graphene on Cu foils of varying thickness (12.5, 25, and 50 μm) also yielded similar graphene structure with regions of double and triple flakes, but neither discontinuous monolayer graphene for thinner Cu foils nor continuous multilayer graphene for thicker Cu foils, as we would have expected based on the precipitation mechanism. According to these observations, we concluded that graphene is growing by a surface-catalyzed process rather than a precipitation process, as has been reported by others for Ni (*5*–*7*). Monolayer graphene formation caused by surface segregation or surface adsorption of carbon has also been observed on transition metals such as Ni and Co at elevated temperatures by Blakely and coauthors (*20*–*22*). However, when the metal substrates were cooled down to room temperature, thick graphite films were obtained because of precipitation of excess C from these metals, in which the solubility of C is relatively high.

In recent work, thin Ni films and a fast-cooling process have been used to suppress the amount of precipitated C. However, this process still yields films with a wide range of graphene layer thicknesses, from one to a few tens of layers and with defects associated with fast cooling (*5*–*7*). Our results suggest that the graphene growth process is not one of C precipitation but rather a CVD process. The precise mechanism will require additional experiments to understand in full, but very low C solubility in Cu (*23*–*25*) and poor C saturation as a result of graphene surface coverage may be playing a role in limiting or preventing the precipitation process altogether at high temperature, similar to the case of impeding of carburization of Ni (*26*). This provides a pathway for growing self-limited graphene films.

To evaluate the electrical quality of the synthesized graphene, we fabricated dual-gated FETs with Al_2O_3 as the gate dielectric and measured them at room temperature. Along with a device model that incorporates a finite density at the Dirac point, the dielectric, and the quantum capacitances (*9*), the data are shown in Fig. 3. The extracted carrier mobility for this device is ~4050 $cm^2 V^{-1} s^{-1}$, with the residual carrier concentration at the Dirac point of $n_0 = 3.2 \times 10^{11}$ cm^{-2}. These data suggest that the films are of reasonable quality, at least sufficient to continue improving the growth process to achieve a material quality equivalent to the exfoliated natural graphite.

References and Notes

1. A. K. Geim, K. S. Novoselov, *Nat. Mater.* **6**, 183 (2007).
2. C. Berger *et al.*, *Science* **312**, 1191 (2006); published online 12 April 2006 (10.1126/science.1125925).
3. K. V. Emtsev *et al.*, *Nat. Mater.* **8**, 203 (2009).
4. P. W. Sutter, J.-I. Flege, E. A. Sutter, *Nat. Mater.* **7**, 406 (2008).
5. Q. Yu *et al.*, *Appl. Phys. Lett.* **93**, 113103 (2008).
6. K. S. Kim *et al.*, *Nature* **457**, 706 (2009).
7. A. Reina *et al.*, *Nano Lett.* **9**, 30 (2009).
8. J. Coraux, A. T. N'Diaye, C. Busse, T. Michely, *Nano Lett.* **8**, 565 (2008).
9. S. Kim *et al.*, *Appl. Phys. Lett.* **94**, 062107 (2009).
10. M. C. Lemme *et al.*, *Solid-State Electron.* **52**, 514 (2008).
11. S. K. Banerjee, L. F. Register, E. Tutuc, D. Reddy, A. H. MacDonald, *IEEE Electron Device Lett.* **30**, 158 (2009).
12. P. Blake *et al.*, *Nano Lett.* **8**, 1704 (2008).
13. R. R. Nair *et al.*, *Science* **320**, 1308 (2008); published online 3 April 2008 (10.1126/science.1156965).
14. X. Wang, L. Zhi, K. Müllen, *Nano Lett.* **8**, 323 (2008).
15. See supporting material on *Science* Online.
16. A. Reina *et al.*, *J. Phys. Chem. C* **112**, 17741 (2008).
17. Z. H. Ni *et al.*, *Nano Lett.* **7**, 2758 (2007).
18. A. C. Ferrari *et al.*, *Phys. Rev. Lett.* **97**, 187401 (2006).
19. A. Das *et al.*, *Nat. Nanotechnol.* **3**, 210 (2008).
20. M. Eizenberg, J. M. Blakely, *Surf. Sci.* **82**, 228 (1979).
21. M. Eizenberg, J. M. Blakely, *J. Chem. Phys.* **71**, 3467 (1979).
22. J. C. Hamilton, J. M. Blakely, *Surf. Sci.* **91**, 199 (1980).
23. R. B. McLellan, *Scr. Metal.* **3**, 389 (1969).
24. G. Mathieu, S. Guiot, J. Carbané, *Scr. Metal.* **7**, 421 (1973).
25. G. A. López, E. J. Mittemeijer, *Scr. Mater.* **51**, 1 (2004).
26. R. Kikowatz, K. Flad, G. Horz, *J. Vac. Sci. Technol. A* **5**, 1009 (1987).

27. We thank the Nanoelectronic Research Initiative (NRI–Southwest Area Nanoelectronics Center, grant no. 2006-NE-1464), the Defense Advanced Research Projects Agency Carbon Electronics for RF Applications Center, and the University of Texas at Austin for support.

Supporting Online Material

www.sciencemag.org/cgi/content/full/1171245/DC1
Materials and Methods
Figs. S1 to S3

22 January 2009; accepted 9 April 2009
Published online 7 May 2009;
10.1126/science.1171245
Include this information when citing this paper.

Downloaded from www.sciencemag.org on October 12, 2010

Superconductivity at the Two-Dimensional Limit

Shengyong Qin, Jungdae Kim, Qian Niu, Chih-Kang Shih*

Superconductivity in the extreme two-dimensional limit is studied on ultrathin lead films down to two atomic layers, where only a single channel of quantum well states exists. Scanning tunneling spectroscopy reveals that local superconducting order remains robust until two atomic layers, where the transition temperature abruptly plunges to a lower value, depending sensitively on the exact atomic structure of the film. Our result shows that Cooper pairs can still form in the last two-dimensional channel of electron states, although their binding is strongly affected by the substrate.

Studies of two-dimensional (2D) superconductivities have been generally limited to the regime where the superconducting order parameter behaves as a 2D wave function but the underline electrons are still three-dimensional (*1*–*11*). Recent advancements in materials synthesis have enabled the growth of epitaxial superconductor thin films with unprec-